

## Effect of Polyampholyte Net Charge on Complex Coacervation between Polyampholytes and Inorganic Polyoxometalate Giant Anions

Manuela Ferreira,<sup>#</sup> Benxin Jing,<sup>#</sup> Adrian Lorenzana, and Yingxi Zhu<sup>\*</sup>

Department of Chemical Engineering and Materials Science,  
Wayne State University, Detroit, MI 48202

<sup>#</sup> M. F. and B.J. equally contributed to this work

<sup>\*</sup>Corresponding author (yzhu3@wayne.edu)

### Supporting Information

**Figure S1. a)** pH-dependent UV-vis spectra of (i) 10  $\mu\text{M}$  free fluorescein and (ii) 10 g/L  $f\text{-PA}_x\text{M}_y$  in buffer solutions of varied pH=2-10. The dash line indicates the location of primary UV-Vis absorbance peak,  $\text{Abs}_{500}$ , which shifts from 490 nm for the case of free fluorescein to 500 nm for  $f\text{-PA}_x\text{M}_y$  due to local environment change. **b)** pH-dependent UV-vis absorbance at absorption peak of 500 nm wavelength,  $\text{Abs}_{500}$  (490 nm for free fluorescein) at  $C_{KCl} = 0.1\text{M}$  for free fluorescein (black squares),  $f\text{-PA}_{45}\text{M}_{55}$  (red circles), and  $f\text{-PA}_{55}\text{M}_{45}$  (blue triangles).

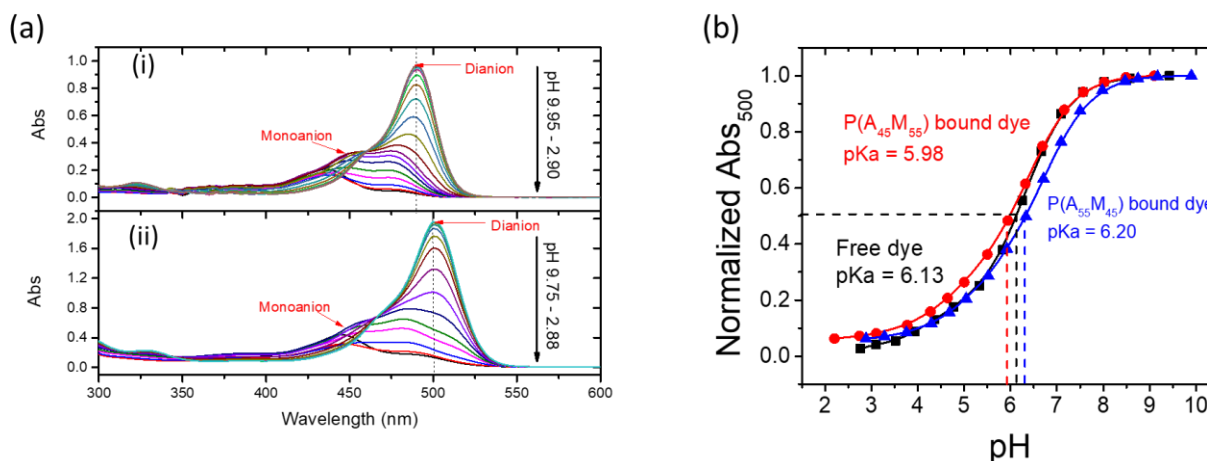


**Figure S2.** Fluorescence micrographs of the morphology of PA<sub>50</sub>M<sub>50</sub> – {W<sub>12</sub>} dense coacervates formed at  $C_{A_xM_y} = 89.6$  mM,  $C_{e^-(W_{12})}/C_{A_xM_y} = 60\%$ , and  $C_{LiCl} = 0.2$  M, after repeat centrifugation to thoroughly remove the supernatant solution.

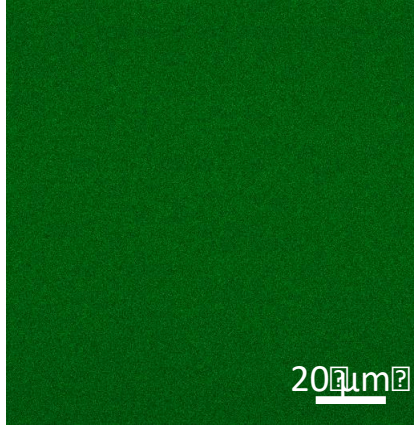


**Figure S3.** Linear frequency-dependent shear spectra of measured elastic moduli,  $G'$  (solid symbols) and viscous moduli,  $G''$  (open symbols) of PA<sub>x</sub>M<sub>y</sub> – {W<sub>12</sub>} dense coacervates formed at constant  $C_{A_xM_y} = 89.6$  mM,  $C_{e^-(W_{12})}/C_{A_xM_y} = 60\%$ , and  $C_{LiCl} = 0.2$  M at constant strain  $\gamma = 1\%$  against  $\omega$  at varied temperature, T = 2 °C (pink stars), 10 °C (green hexagons), 22 °C (magenta diamonds), 30 °C (blue triangles), 42 °C (red circles), and 58 °C (black squares) for (a) PA<sub>45</sub>M<sub>55</sub>, (b) PA<sub>50</sub>M<sub>50</sub>, and (c) PA<sub>55</sub>M<sub>45</sub>.

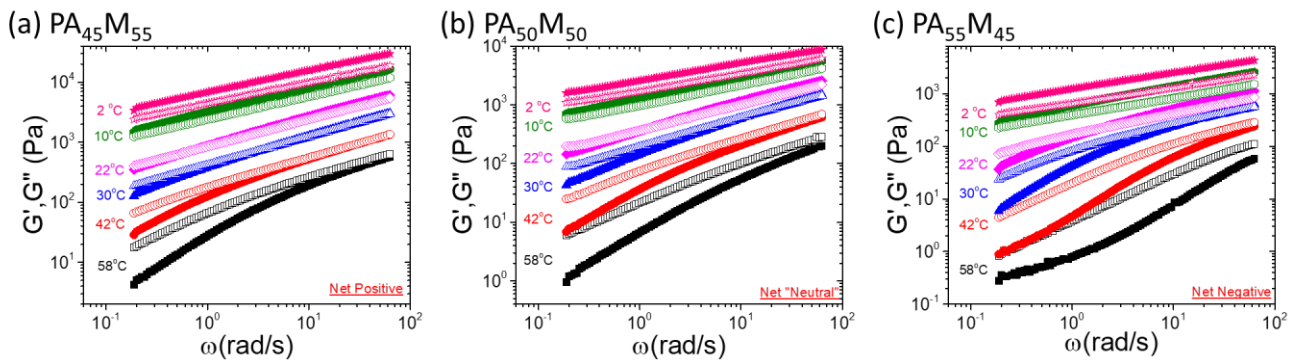


**Figure S4.** Temperature-dependent shift factor,  $a_T$ , from the time-temperature superimposition of the linear shear spectra of  $PA_xM_y - \{W_{12}\}$  dense coacervates with  $PA_{45}M_{55}$  (black squares),  $PA_{50}M_{50}$  (red circles), and  $PA_{55}M_{45}$  (blue triangles) as shown in Figure S3a-c, respectively, where  $T_r = 22^\circ\text{C}$  is the room temperature, thus selected as the reference temperature in this work.

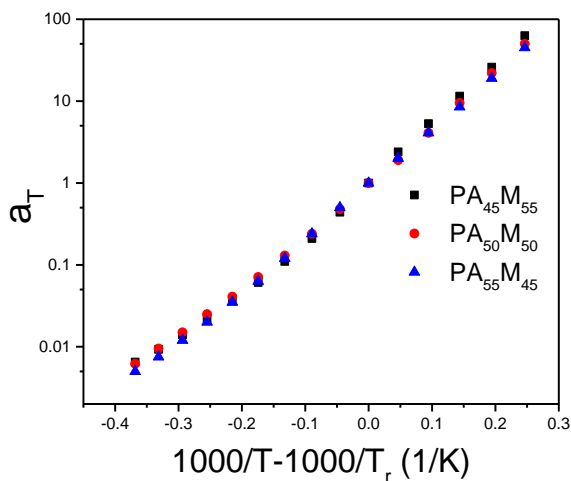


**Figure S5.** Time-temperature superposition master curves of shear moduli  $G'$  (solid symbol),  $G''$  (open symbol) of (a)  $PA_{45}M_{55} - \{W_{12}\}$  and (b)  $PA_{50}M_{50} - \{W_{12}\}$  gel against shifted angular frequency,  $\omega a_T$  for the complexes formed at constant  $C_{A_xM_y} = 89.6 \text{ mM}$ ,  $C_{e^- (W_{12})} / C_{A_xM_y} = 1200\%$ , and  $C_{LiCl} = 0.2 \text{ M}$  at constant strain  $\gamma = 1\%$ . Linear shear spectra were obtained at varied  $T = 2\text{-}58^\circ\text{C}$  and  $T_r = 22^\circ\text{C}$  is selected for time-temperature superposition analysis.

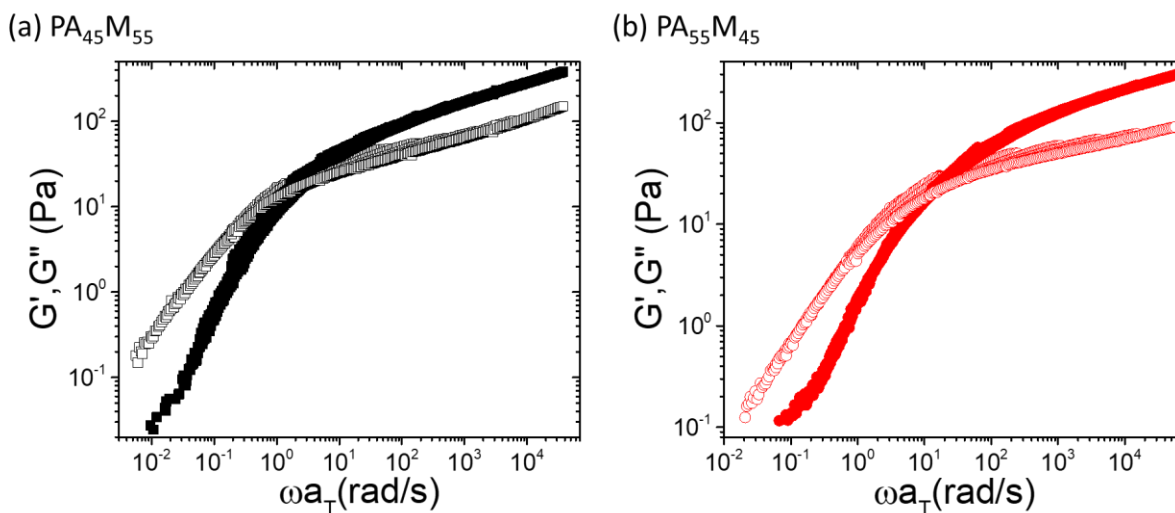


**Figure S6.** Linear frequency-dependent shear spectra of measured elastic moduli,  $G'$  (solid symbols) and viscous moduli,  $G''$  (open symbols) of  $PA_xM_y - \{W_{12}\}$  dense coacervates formed at constant  $C_{A_xM_y} = 89.6$  mM and  $C_{LiCl} = 0.2$  M at constant temperature of 22 °C and strain  $\gamma = 1\%$  against  $\omega$  for (a)  $PA_{45}M_{55}$ , (b)  $PA_{50}M_{50}$ , and (c)  $PA_{55}M_{45}$  at varied  $C_{e^-(W_{12})}/C_{A_xM_y}$ .

